

Window Designs for DFT-Based Multicarrier Systems

Yuan-Pei Lin, *Senior Member, IEEE*, and See-May Phoong, *Senior Member, IEEE*

Abstract—In this paper, we consider window designs for discrete Fourier transform (DFT) based multicarrier transceivers without using extra cyclic prefix. As in previous works of window designs for DFT-based transceivers, a postprocessing matrix that is generally channel dependent, is needed to have a zero-forcing receiver. We show that postprocessing is channel independent if and only if the window itself has the cyclic-prefixed property. We design optimal windows with minimum spectral leakage subject to the cyclic-prefixed condition. Moreover, we analyze how postprocessing affects the signal-to-noise ratio (SNR) at the receiver, which is an aspect that is not considered in most of the earlier works. The resulting SNR can be given in a closed form. Joint optimization of spectral leakage and SNR are also considered. Furthermore, examples demonstrate that we can have a significant reduction in spectral leakage at the cost of a small SNR loss. In addition to cyclic-prefixed systems, window designs for zero-padded DFT-based transceivers are considered. For the zero-padded transceivers, windows that minimize spectral leakage can also be designed.

Index Terms—DMT, egress control, multicarrier, PSD mask, window.

I. INTRODUCTION

DISCRETE Fourier transform (DFT) based multicarrier systems have found applications in a wide range of transmission systems, e.g., discrete multitone (DMT) for asymmetric digital subscriber lines (ADSLs) [2], very high speed digital subscriber lines (VDSLs) [3], and orthogonal frequency division multiplexing (OFDM) for wireless local area networks (LANs) [4] and digital video broadcasting (DVB) [5]. The transmitter and receiver perform, respectively, M -point IDFT (inverse DFT) and DFT computation, where M is the number of subchannels. At the transmitter side, each block is padded with cyclic prefix of length L . The number L is chosen to be no smaller than the order of the channel, which is usually assumed to be a finite impulse response (FIR) filter. Using redundant cyclic prefix, intersymbol interference (ISI) is canceled completely. As a result, an FIR channel is converted into M subchannels. The subchannel gains are the M -point DFT of the FIR channel impulse response.

Manuscript received May 14, 2003; revised March 17, 2004. The work was supported in part by the NSC under Grants 90-2213-E-009-108 and 90-2213-E-002-097, the Ministry of Education under Contract 89-E-FA06-2-4, Taiwan, R.O.C., and the Lee and MTI Center for Networking Research. The associate editor coordinating the review of this manuscript and approving it for publication was Dr. Ta-Hsin Li.

Y.-P. Lin is with the Department of Electrical and Control Engineering, National Chiao Tung University, Hsinchu, Taiwan, R.O.C. (e-mail: ypl@cc.nctu.edu.tw).

S.-M. Phoong is with the Department of Electrical Engineering and Graduate Institute of Communications Engineering, National Taiwan University, Taipei, Taiwan, R.O.C.

Digital Object Identifier 10.1109/TSP.2004.842173

In the conventional DFT-based multicarrier system the pulse shaping filter is a rectangular window. As a rectangular window has large spectral sidelobes, there is a large spectral leakage. This could pose a problem in applications where the power spectral density (PSD) of the transmit signal is required to have a large rolloff in certain frequency bands. For example, in some wired transmission application, the PSD of the downstream transmit signal needs to fall below a threshold in the frequency bands of upstream transmission to avoid interference [2], [3]. The PSD should also be attenuated in amateur radio bands to reduce interference or egress emission [3].

Many methods have been proposed to reduce sidelobes by windowing, filtering, or using different pulse-shaping filters. A number of nonrectangular continuous-time pulse shapes have been proposed to improve the spectral rolloff of the transmit signal, e.g., [6]–[9]. It is demonstrated in [10] that OFDM systems with nonrectangular continuous-time pulse shaping filters can be represented by a shaping matrix followed by the usual analog transmitter. Usually, continuous-time pulse shapes are designed based on analog implementation of OFDM transmitters, and these pulses usually do not admit a digital implementation [11]. Discrete-time windows that can be easily incorporated in digital transmitters implementation have been considered in [12]–[14]. In [12], overlapping windows of duration longer than one OFDM symbol is proposed to reduce spectral sidelobes. In this case, significant ISI is generated even if the channel does not introduce ISI, and an additional postprocessing equalizer is used to remove ISI. The design of overlapping windows for OFDM with offset quadrature amplitude modulation (QAM) over distortion-less channels are studied fully in [13] and [14]. When the channel is distortion-less, orthogonality among the subchannels is preserved [13], [14], and a better spectral efficiency is achieved.

However, for channels with distortion, i.e., ISI channels, the subchannel outputs contain intra- and inter-subchannel interference; additional processing is required to remove interference in this case. If extra guard time is available, postprocessing can be avoided at the cost of a reduced transmission rate [15]. When there is no extra cyclic prefix, the use of windowing at the transmitter requires postprocessing at the receiver. More recently, transmitting windows with the cyclic-prefixed property have been proposed in [16] for egress control. Windows that are the inverse of a raised cosine function are optimized to minimize spectral leakage and, hence, minimize egress emission. The corresponding zero-forcing receiver also requires postprocessing equalization.

In this paper, we will consider window designs for DFT-based multicarrier system without using extra cyclic prefix. Windowed transceivers with both cyclic prefix and zero padding will be considered for ISI channels. For the cyclic-prefixed case, post-

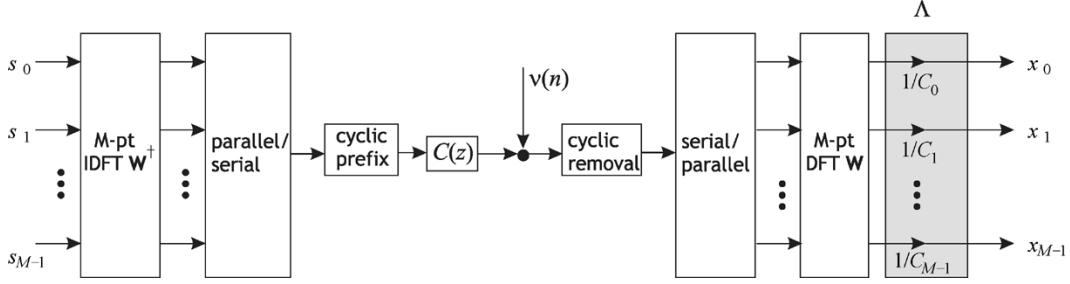


Fig. 1. Cyclic-prefixed DFT-based multicarrier system over a channel $C(z)$ with additive noise $v(n)$.

processing is, in general, channel dependent. We will derive the explicit dependency on the channel and show that the postprocessing matrix that cancels ISI at the output of the receiver is channel independent if the window itself has the cyclic-prefixed property. In this case, the output of the transmitter has the usual cyclic-prefixed property. Techniques that exploit cyclic prefix for synchronization can still be used. We will design windows that minimize spectral leakage subject to the cyclic-prefixed constraint.

Moreover, we show that postprocessing can affect the SNR at the receiver, which is an aspect mostly overlooked in earlier window designs for DFT-based transceivers. We will see that the resulting SNR can be given in a closed form in terms of the transmit window if the channel noise is additive white Gaussian noise (AWGN). Furthermore, joint optimization of spectral leakage and SNR can be achieved by using an objective function that incorporates both terms. Examples will be given to demonstrate that a good tradeoff between spectral rolloff and SNR can be obtained through such an optimization. For the zero padding case, we will see that the postprocessing matrix depends on the window only but not on the channel. The output SNR, unlike the cyclic prefix case, depends on the window as well as the channel. A lower bound and an upper bound can be found for the SNR at the receiver. As in the cyclic prefix case, we design optimal windows that minimize the spectral leakage. The window can also be designed by jointly optimizing the SNR and spectral leakage.

The sections are organized as follows. In Section II, we consider windowed transceivers with cyclic prefix and derive the receiver for a given window. The zero padding case is considered in Section III. The design method and examples of windowed systems will be given in Section IV.

Notations and Preliminaries:

- 1) Boldfaced lowercase letters are used to represent vectors, and boldfaced uppercase letters are reserved for matrices. The notation \mathbf{A}^\dagger denotes transpose-conjugate of \mathbf{A} .
- 2) The function $E[y]$ denotes the expected value of the random variable y .
- 3) The notation \mathbf{I}_M is used to represent the $M \times M$ identity matrix. The subscript is omitted whenever the size is clear from the context.
- 4) The notation $\text{diag}(\lambda_0 \lambda_1 \cdots \lambda_{M-1})$ denotes an $M \times M$ diagonal matrix with the k th diagonal element equal to λ_k .

- 5) The notation \mathbf{W} is used to represent the $M \times M$ orthogonal DFT matrix given by

$$[\mathbf{W}]_{kn} = \frac{1}{\sqrt{M}} e^{-j \frac{2\pi}{M} kn}, \quad \text{for } 0 \leq k, n \leq M-1.$$

- 6) An $M \times M$ matrix \mathbf{C} is called a circulant matrix if it is of the form

$$\mathbf{C} = \begin{pmatrix} c_0 & c_{M-1} & c_{M-2} & \cdots & c_1 \\ c_1 & c_0 & c_{M-1} & & c_2 \\ c_2 & c_1 & c_0 & & c_3 \\ \vdots & & & \ddots & \vdots \\ c_{M-1} & c_{M-2} & c_{M-3} & \cdots & c_0 \end{pmatrix}. \quad (1)$$

It is known that an $M \times M$ circulant matrix can be diagonalized using $M \times M$ DFT matrices. In particular, the matrix \mathbf{C} can be expressed as

$$\mathbf{C} = \mathbf{W}^\dagger \mathbf{\Gamma} \mathbf{W} \quad (2)$$

where $\mathbf{\Gamma}$ is a diagonal matrix, whose M diagonal elements are the M -point DFT of the sequence $\{c_0, c_1, \dots, c_{M-1}\}$. That is, $[\mathbf{\Gamma}]_{ii} = \sum_{k=0}^{M-1} c_k e^{-jki2\pi/M}$. Conversely, any matrix of the form in (2) is a circulant matrix.

II. DFT-BASED TRANSCIVERS WITH CYCLIC PREFIX

In this section, we consider windowed DFT-based transceivers with cyclic prefix. The block diagram of the DFT-based transceivers with cyclic prefix is as shown in Fig. 1. The modulation symbols to be transmitted are first blocked into M by 1 vectors, where M is the number of subchannels. The input symbols s_k are passed through an M by M IDFT matrix, followed by the parallel-to-serial (P/S) operation and the insertion of cyclic prefix. The length of the cyclic prefix L is chosen to be equal to or larger than the order of the channel $C(z)$. At the receiver, the cyclic prefix is discarded, and the samples are again blocked into M by 1 vectors for M -point DFT computation. The scalar multipliers $1/C_k$ are also called frequency domain equalizers, where C_0, C_1, \dots, C_{M-1} are the M -point DFT of the channel impulse response c_n . The prefix is discarded at the receiver to remove interblock interference. The transceiver is ISI free and the receiver is a zero-forcing receiver.

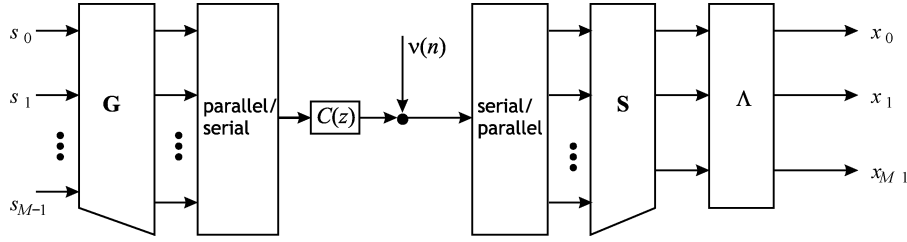


Fig. 2. Block-based representation of the transceiver in Fig. 1.

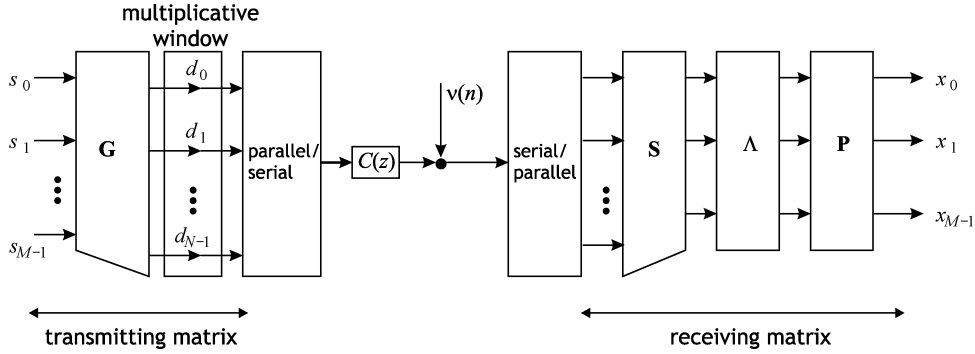


Fig. 3. Windowed DFT-based transceiver.

A. System Model

The transceiver in Fig. 1 can be redrawn as in Fig. 2. The matrices \mathbf{G} and \mathbf{S} shown in Fig. 2 are of dimensions $N \times M$ and $M \times N$, where $N = M + L$. They are given, respectively, by

$$\mathbf{G}_{\text{cp}} = \begin{pmatrix} \mathbf{0} & \mathbf{I}_L \\ \mathbf{I}_M & \mathbf{0} \end{pmatrix} \mathbf{W}^\dagger, \quad \text{and} \quad \mathbf{S}_{\text{cp}} = \mathbf{W} \begin{pmatrix} \mathbf{0} & \mathbf{I} \end{pmatrix} \quad (3)$$

where we have used the subscript ‘‘cp’’ to highlight that these matrices are for the case of cyclic prefix. The matrix $\mathbf{\Lambda}$ indicated in Fig. 2 is diagonal and given by

$$\mathbf{\Lambda} = \text{diag} \left(\frac{1}{C_0}, \frac{1}{C_1}, \dots, \frac{1}{C_{M-1}} \right).$$

We can obtain a windowed system by applying a window to each transmitter output block, as shown in Fig. 3. The length of the window is the same as the block length N . The window has coefficients d_0, d_1, \dots, d_{N-1} , with z-transform $D(z)$. The conventional system in Fig. 2 can be viewed as having a rectangular window with length N . Due to the nonrectangular window at the transmitter, the receiver needs an additional postprocessing matrix \mathbf{P} to cancel intersubchannel interference. As there is no constraint on the matrix \mathbf{P} , there is no loss of generality in considering the receiver of the form shown in Fig. 3. The transmitting matrix can be written as $\mathbf{D}_{\text{cp}} \mathbf{G}_{\text{cp}}$, where \mathbf{D}_{cp} is the diagonal matrix

$$\mathbf{D}_{\text{cp}} = \text{diag}(d_0 \ d_1 \ \dots \ d_{N-1}). \quad (4)$$

We partition \mathbf{D} as

$$\mathbf{D}_{\text{cp}} = \begin{pmatrix} \mathbf{D}_0 & \mathbf{0} & \mathbf{0} \\ \mathbf{0} & \mathbf{D}_1 & \mathbf{0} \\ \mathbf{0} & \mathbf{0} & \mathbf{D}_2 \end{pmatrix}$$

where \mathbf{D}_0 and \mathbf{D}_2 are of dimensions $L \times L$, and \mathbf{D}_1 is of dimensions $(M - L) \times (M - L)$. For a given window, we now derive the condition on \mathbf{P} so that the overall system is ISI free.

Lemma 1: Consider the DFT-based transceiver with cyclic prefix in Fig. 3. The receiver is zero forcing if and only if the postprocessing matrix \mathbf{P} is given by

$$\mathbf{P}_{\text{cp}} = \left[\mathbf{W} \begin{pmatrix} \mathbf{D}_1 & \mathbf{0} \\ \mathbf{0} & \mathbf{D}_2 \end{pmatrix} \mathbf{W}^\dagger + \mathbf{\Lambda} \mathbf{W} \begin{pmatrix} \mathbf{0} & \mathbf{C}_2(\mathbf{D}_0 - \mathbf{D}_2) \\ \mathbf{0} & \mathbf{0} \end{pmatrix} \mathbf{W}^\dagger \right]^{-1} \quad (5)$$

where \mathbf{C}_2 is an L by L lower triangle Toeplitz matrix with the first column given by $(c_0 \ c_1 \ \dots \ c_{L-1})^T$.

A proof is given in the Appendix.

From the above lemma, we see that the solution of the postprocessing matrix depends on the window \mathbf{D} as well as the channel. This channel dependency means that \mathbf{P}_{cp} needs to be computed along with other channel-dependent parameters. To remove such a dependency, we observe that \mathbf{P}_{cp} is channel independent if $\mathbf{D}_0 = \mathbf{D}_2$. That is, the window itself has the cyclic-prefixed property. In this case, the postprocessing matrix is given by

$$\mathbf{P}_{\text{cp}} = \mathbf{W} \text{diag} \left(\frac{1}{d_L}, \frac{1}{d_{L+1}}, \dots, \frac{1}{d_{N-1}} \right) \mathbf{W}^\dagger. \quad (6)$$

Notice that to have a channel-independent \mathbf{P}_{cp} for any channel, the condition $\mathbf{D}_0 = \mathbf{D}_2$ is not only sufficient but also necessary.

Spectral Leakage: Let $D(e^{j\omega})$ denote the Fourier transform of the window function. The stopband energy of the window is

$$\mathcal{S} = \int_{\omega_s}^{2\pi - \omega_s} |D(e^{j\omega})|^2 \frac{d\omega}{2\pi} \quad (7)$$

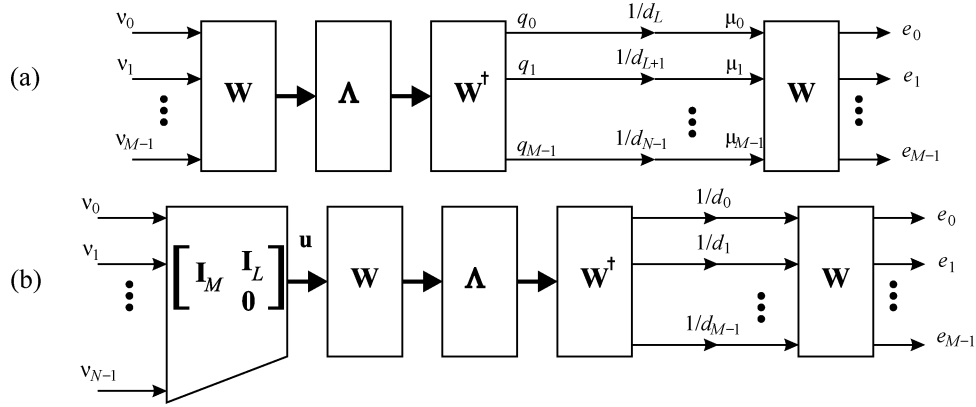


Fig. 4. Noise path at the receiver for (a) the cyclic prefix case and (b) the zero padding case.

where $\omega_s = 2\pi/N$. We define the spectral leakage β_{cp} as

$$\beta_{cp} \triangleq \frac{\mathcal{S}_{d,cp}}{\mathcal{S}_{rec,cp}} \quad (8)$$

where \mathcal{S}_{rec} is the stopband energy of the rectangular window, and $\mathcal{S}_{d,cp}$ is the stopband energy of the window \mathbf{d} . In Section IV, we will see how to design windows that improve the spectral leakage of the window subject to the cyclic prefix condition.

B. Noise Analysis

We assume that the window has the cyclic-prefixed property and the postprocessing matrix is channel independent as given in (6). Suppose the channel noise $\nu(n)$ is AWGN with variance \mathcal{N}_0 . We constrain the transmission power to be the same as the conventional system with a rectangular window. That is, the window satisfies the condition

$$\frac{1}{N} \sum_{k=0}^{N-1} |d_k|^2 = 1. \quad (9)$$

Fig. 4(a) shows the noise path for the windowed system. The input noise vector \mathbf{v} is a block of M Gaussian random variables drawn from the channel noise process $\nu(n)$. The autocorrelation matrix of the noise vector \mathbf{q} is given by

$\mathbf{R}_q = \mathcal{N}_0 \mathbf{W}^\dagger \mathbf{\Lambda} \mathbf{\Lambda}^\dagger \mathbf{W}$, where

$$\mathbf{\Lambda} = \text{diag} \left(\frac{1}{C_0} \quad \frac{1}{C_1} \quad \cdots \quad \frac{1}{C_{M-1}} \right).$$

From the above equation, we know that \mathbf{R}_q is a circulant matrix; all the elements in \mathbf{q} has the same variance σ_q^2 equal to

$$\sigma_q^2 = \frac{\mathcal{N}_0}{M} \sum_{i=0}^{M-1} \frac{1}{|C_i|^2}.$$

Therefore, μ_k , as indicated in Fig. 4(a), has variance $\sigma_{\mu_k}^2 = \sigma_q^2 / |d_{k+L}|^2$. As the DFT matrix \mathbf{W} preserves power, the total output noise power $\mathcal{E}_{d,cp}$ is the sum of all $\sigma_{\mu_k}^2$. That is

$$\mathcal{E}_{d,cp} = \sigma_q^2 \sum_{k=L}^{N-1} \frac{1}{|d_k|^2} = \frac{\mathcal{N}_0}{M} \left[\sum_{i=0}^{M-1} \frac{1}{|C_i|^2} \right] \left[\sum_{k=0}^{M-1} \frac{1}{|d_k|^2} \right] \quad (10)$$

where we have used the cyclic-prefixed property of the window.

In the conventional system, the window is rectangular with $d_k = 1$, for $k = 0, 1, \dots, M-1$. The total output noise power in this case is simply

$$\mathcal{E}_{rec,cp} = \mathcal{N}_0 \sum_{i=0}^{M-1} \frac{1}{|C_i|^2}. \quad (11)$$

To compare the output noise with the conventional system with rectangular window for the same signal variance, we define the quantity SNR loss $\alpha_{cp} = \mathcal{E}_{d,cp} / \mathcal{E}_{rec,cp}$. Using (10) and (11), we have

$$\alpha_{cp} = \frac{1}{M} \sum_{k=0}^{M-1} \frac{1}{|d_k|^2}. \quad (12)$$

III. DFT-BASED TRANSCIVERS WITH ZERO PADDING

In a DFT-based transceiver with zero padding, for each block of size M to be transmitted, L zeros, instead of cyclic prefix, are padded. The zero-padded system can also be represented using the block-based transceiver in Fig. 2. Now, the matrices \mathbf{G} and \mathbf{S} in Fig. 2 are given by

$$\mathbf{G}_{zp} = \begin{pmatrix} \mathbf{W}^\dagger \\ \mathbf{0} \end{pmatrix}, \quad \mathbf{S}_{zp} = \mathbf{W} \begin{pmatrix} \mathbf{I}_M & \mathbf{I}_L \\ \mathbf{0} & \mathbf{0} \end{pmatrix}.$$

We can obtain a windowed system with zero padding from Fig. 3 by setting the last L window coefficients to zero. In this case, the transmitting matrix can be expressed as $(\mathbf{D}_{zp} \mathbf{W}^\dagger)$, where \mathbf{D}_{zp} is an $M \times M$ diagonal matrix with $\mathbf{D}_{zp} = \text{diag}(d_0, d_1, \dots, d_{M-1})$. The window has M coefficients, d_0, d_1, \dots, d_{M-1} . The window is constrained to satisfy $1/M \sum_{k=0}^{M-1} |d_k|^2 = 1$ so that it has the same transmission power as the zero-padded system with a rectangular window.

Lemma 2: Consider the DFT-based transceiver with zero padding. For a given transmit window, the receiver is zero forcing if and only if the postprocessing matrix \mathbf{P} is given by

$$\mathbf{P}_{zp} = \mathbf{W} \mathbf{D}_{zp}^{-1} \mathbf{W}^\dagger.$$

Proof: As there is no interblock interference, the overall transfer function is

$$\mathbf{T} = \mathbf{P}_{\text{zp}} \mathbf{A} \mathbf{W} \underbrace{\begin{pmatrix} \mathbf{I}_M & \mathbf{I}_L \\ & \mathbf{0} \end{pmatrix}}_{\mathbf{C}} \mathbf{B} \mathbf{D}_{\text{zp}} \mathbf{W}^\dagger$$

where \mathbf{B} is an $N \times M$ Toeplitz matrix with the first column given by $(c_0 \ c_1 \ \dots \ c_L \ 0 \ \dots \ 0)^T$. The matrix \mathbf{C} , indicated in the above equation, is circulant, as in (1). Using $\mathbf{C} = \mathbf{W}^\dagger \mathbf{\Gamma} \mathbf{W}$ in (2) and $\mathbf{\Gamma} = \mathbf{\Lambda}^{-1}$, we arrive at

$$\mathbf{T} = \mathbf{P}_{\text{zp}} \mathbf{W} \mathbf{D}_{\text{zp}} \mathbf{W}^\dagger.$$

The receiver is zero-forcing solution, i.e., $\mathbf{T} = \mathbf{I}$, if and only if $\mathbf{P}_{\text{zp}} = \mathbf{W} \mathbf{D}_{\text{zp}}^{-1} \mathbf{W}^\dagger$. $\triangle\triangle\triangle$

Similar to the cyclic-prefixed case, we define the spectral leakage β_{zp} as

$$\beta_{\text{zp}} = \frac{\mathcal{S}_{\text{rec,zp}}}{\mathcal{S}_{\text{d,zp}}}$$

where $\mathcal{S}_{\text{rec,zp}}$ is the stopband energy of the rectangular window with length M . The expression is exactly as in (7). The only difference is that the window is now a window of M coefficients. For a given window, we can also compute the total output noise power $\mathcal{E}_{\text{d,zp}}$, as in the cyclic prefix case. We can also define the SNR loss as the ratio of the total output noise power of the windowed system over that of the zero-padded DFT-based transceiver with a rectangular window

$$\alpha_{\text{zp}} \triangleq \frac{\mathcal{E}_{\text{d,zp}}}{\mathcal{E}_{\text{rec,zp}}}$$

The total output noise power for a given window \mathbf{d} is given in the following lemma.

Lemma 3: Consider the windowed DFT-based transceiver system with zero padding in Fig. 3. The channel noise is AWGN with variance \mathcal{N}_0 . The total output noise power is given by

$$\mathcal{E}_{\text{d,zp}} = \frac{\mathcal{N}_0}{M} \sum_{i=0}^{M-1} \frac{1}{|d_i|^2} \sum_{k=0}^{M-1} \frac{1}{|C_k|^2} + \mathcal{N}_0 \sum_{i=0}^{L-1} [\mathbf{A}^\dagger \mathbf{A}]_{ii}$$

where $\mathbf{A} = \mathbf{W} \mathbf{D}_{\text{zp}}^{-1} \mathbf{W}^\dagger \mathbf{\Lambda} \mathbf{W}$. (13)

Proof: Fig. 4(b) shows the noise path at the receiver for the zero-padded system with windowing. The input noise vector $\boldsymbol{\nu}$ is of dimensions $N \times 1$. Let

$$\mathbf{u}_1 = \begin{pmatrix} \mathbf{I}_M & \mathbf{0} \\ & \mathbf{0} \end{pmatrix} \boldsymbol{\nu}, \quad \mathbf{u}_2 = \begin{pmatrix} \mathbf{0} & \mathbf{I}_L \\ & \mathbf{0} \end{pmatrix} \boldsymbol{\nu}.$$

Then, the noise vector \mathbf{u} indicated in Fig. 4(b) is $\mathbf{u} = \mathbf{u}_1 + \mathbf{u}_2$. The output noise vector \mathbf{e} can be expressed as

$$\mathbf{e} = \underbrace{\mathbf{A} \mathbf{u}_1}_{\mathbf{e}_1} + \underbrace{\mathbf{A} \mathbf{u}_2}_{\mathbf{e}_2}$$

where $\mathbf{A} = \mathbf{W} \mathbf{D}_{\text{zp}}^{-1} \mathbf{W}^\dagger \mathbf{\Lambda} \mathbf{W}$, as given in (13). As \mathbf{u}_1 and \mathbf{u}_2 are uncorrelated, the two noise vectors \mathbf{e}_1 and \mathbf{e}_2 are uncorrelated as well; the output noise power $\mathcal{E}_{\text{d,zp}} = E[\mathbf{e}^\dagger \mathbf{e}]$ can be computed by adding together $E[\mathbf{e}_1^\dagger \mathbf{e}_1]$ and $E[\mathbf{e}_2^\dagger \mathbf{e}_2]$. The noise vector \mathbf{u}_1 is

obtained by blocking the channel noise, and the noise transfer function is similar to that of the cyclic prefix case. The noise variance $E[\mathbf{e}_1^\dagger \mathbf{e}_1]$ can be computed using the technique for the cyclic prefix case, and we have

$$E[\mathbf{e}_1^\dagger \mathbf{e}_1] = \frac{\mathcal{N}_0}{M} \left[\sum_{i=0}^{M-1} \frac{1}{|C_i|^2} \right] \left[\sum_{k=0}^{M-1} \frac{1}{|d_k|^2} \right].$$

On the other hand, we notice that the elements of \mathbf{u}_2 are uncorrelated. Let \mathbf{y}_i be an $M \times 1$ column vector whose i th element is equal to $[\mathbf{u}_2]_i$, and all the other elements are zero for $i = 0, 1, \dots, L-1$. That is, \mathbf{y}_i for $i = 0, 1, \dots, L-1$ is given by $[\mathbf{y}_i]_j = [\mathbf{u}_2]_i \delta(i-j)$, for $j = 0, 1, \dots, M-1$. Then, $\mathbf{u}_2 = \sum_{i=0}^{L-1} \mathbf{y}_i$, and therefore, \mathbf{e}_2 can be expressed as

$$\mathbf{e}_2 = \sum_{i=0}^{L-1} \underbrace{\mathbf{A} \mathbf{y}_i}_{\mathbf{f}_i} = \sum_{i=0}^{L-1} \mathbf{f}_i.$$

Note that \mathbf{y}_i has only one nonzero element, and hence, $E[\mathbf{f}_i^\dagger \mathbf{f}_i] = \mathcal{N}_0 [\mathbf{A}^\dagger \mathbf{A}]_{ii}$. As the elements of \mathbf{u}_2 are uncorrelated, we have $E[\mathbf{e}_2^\dagger \mathbf{e}_2] = \sum_{i=0}^{L-1} E[\mathbf{f}_i^\dagger \mathbf{f}_i]$. Therefore

$$E[\mathbf{e}_2^\dagger \mathbf{e}_2] = \sum_{i=0}^{L-1} \mathcal{N}_0 [\mathbf{A}^\dagger \mathbf{A}]_{ii}.$$

As $E[\mathbf{e}^\dagger \mathbf{e}] = E[\mathbf{e}_1^\dagger \mathbf{e}_1] + E[\mathbf{e}_2^\dagger \mathbf{e}_2]$, we arrive at the expression in (13). $\triangle\triangle\triangle$

The expression in (13) implies $\mathcal{E}_{\text{d,zp}}$ is an increasing function of L ; as L increases, more diagonal terms $\mathcal{N}_0 [\mathbf{A}^\dagger \mathbf{A}]_{ii}$ are added. The value of $\mathcal{E}_{\text{d,zp}}$ attains the maximum when $L = M$ (L is assumed to be $\leq M$). The output noise power $\mathcal{E}_{\text{rec,zp}}$ for the rectangular window case can be obtained by setting $d_0 = d_1 = \dots = d_{M-1} = 1$ in the expression of $\mathcal{E}_{\text{d,cp}}$ in (13). In particular, we can verify that $\mathcal{E}_{\text{rec,zp}}$ is given by

$$\mathcal{E}_{\text{rec,zp}} = \mathcal{N}_0 \frac{N}{M} \sum_{k=0}^{M-1} \frac{1}{|C_k|^2}.$$

From (13), we see that unlike the cyclic prefix case, $\alpha_{\text{zp}} = \mathcal{E}_{\text{d,zp}}/\mathcal{E}_{\text{rec,zp}}$ is a quantity that depends on the channel. The following lemma gives a channel-independent lower and upper bound on α_{zp} . The gap between the lower bound and the upper bound is 3 dB.

Lemma 4: Consider the windowed DFT-based transceiver system with zero padding in Fig. 3. The channel noise is AWGN with variance \mathcal{N}_0 . The total output noise power is bounded as follows:

$$\frac{\mathcal{N}_0}{M} \sum_{i=0}^{M-1} \frac{1}{|d_i|^2} \sum_{k=0}^{M-1} \frac{1}{|C_k|^2} \leq \mathcal{E}_{\text{d,zp}} \leq \frac{2\mathcal{N}_0}{M} \sum_{i=0}^{M-1} \frac{1}{|d_i|^2} \sum_{k=0}^{M-1} \frac{1}{|C_k|^2}. \quad (14)$$

The SNR loss α_{zp} is bounded by

$$\frac{1}{N} \sum_{i=0}^{M-1} \frac{1}{|d_i|^2} \leq \alpha_{\text{zp}} \leq \frac{2}{N} \sum_{i=0}^{M-1} \frac{1}{|d_i|^2} \quad (15)$$

where $N = M + L$.

Proof: From (13), we see the total output noise power $\mathcal{E}_{d, \text{cp}}$ reaches the minimum when $L = 0$ and the maximum when $L = M$. When $L = 0$, $\mathcal{E}_{d, \text{cp}} = (\mathcal{N}_0/M) \sum_{i=0}^{M-1} (1/|d_i|^2) \sum_{k=0}^{M-1} (1/|C_k|^2)$, i.e., the lower bound in (14). When $L = M$, we can follow the procedure in the proof of Lemma 3 to show that $\mathcal{E}_{d, \text{cp}} = (2\mathcal{N}_0/M) \sum_{i=0}^{M-1} (1/|d_i|^2) \sum_{k=0}^{M-1} (1/|C_k|^2)$. Using the bounds of $\mathcal{E}_{d, \text{zP}}$ given in (14), we can obtain the bounds of α_{zP} in (15). $\triangle\triangle\triangle$

IV. WINDOW DESIGNS

In this section, we will design optimal windows for cyclic-prefixed and zero-padded systems to minimize spectral leakage. The use of windows improves the spectral rolloff of the transmitter outputs significantly. We will also optimize both spectral leakage and SNR by considering a joint objective function consisting of both terms. The joint optimization yields a tradeoff between spectral leakage and SNR.

A. Windows for Cyclic-Prefixed Systems

We have shown in Section II that a cyclic-prefixed window yields channel-independent postprocessing. We will design windows for cyclic-prefixed systems subject to this constraint. Let \mathbf{d} be the N by 1 window vector and $\hat{\mathbf{d}} = (d_L \ d_{L+1} \ \dots \ d_{N-1})^T$ be a column vector containing only the last M coefficients of the window. The cyclic-prefixed property means that \mathbf{d} can be written as

$$\mathbf{d} = \mathbf{F}\hat{\mathbf{d}}, \quad \text{where } \mathbf{F} = \begin{pmatrix} \mathbf{0} & \mathbf{I}_L \\ & \mathbf{I}_M \end{pmatrix}.$$

The Fourier transform of the window can be expressed as

$$D(e^{j\omega}) = \mathbf{e}(e^{j\omega})\mathbf{F}\hat{\mathbf{d}}, \quad \text{where} \\ \mathbf{e}(e^{j\omega}) = \begin{pmatrix} 1 & e^{-j\omega} & e^{-j2\omega} & \dots & e^{-j(N-1)\omega} \end{pmatrix}. \quad (16)$$

It follows that the squared magnitude response of the window is

$$|D(e^{j\omega})|^2 = \hat{\mathbf{d}}^\dagger \mathbf{F}^T \underbrace{\mathbf{e}^\dagger(e^{j\omega})\mathbf{e}(e^{j\omega})}_{\mathbf{E}(e^{j\omega})} \mathbf{F}\hat{\mathbf{d}}$$

where $[\mathbf{E}(e^{j\omega})]_{mn} = e^{j\omega(m-n)}$. The stopband energy of the window in (7) can be expressed as

$$\mathcal{S} = \hat{\mathbf{d}}^\dagger \mathbf{F}^T \underbrace{\int_{\omega_s}^{2\pi-\omega_s} \mathbf{E}(e^{j\omega}) \frac{d\omega}{2\pi}}_{\mathbf{Q}} \mathbf{F}\hat{\mathbf{d}} = \hat{\mathbf{d}}^\dagger \mathbf{F}^T \mathbf{Q} \mathbf{F}\hat{\mathbf{d}}. \quad (17)$$

The $N \times N$ matrix \mathbf{Q} is given by

$$[\mathbf{Q}]_{mn} = \int_{\omega_s}^{2\pi-\omega_s} e^{j\omega(m-n)} \frac{d\omega}{2\pi} = \begin{cases} 1 - \frac{\omega_s}{\pi}, & m = n \\ -\frac{\sin(\frac{\pi}{\pi(m-n)}\omega_s)}{\pi(m-n)}, & \text{otherwise.} \end{cases}$$

It is real, symmetric, and positive semi definite.

Using (17), we can see that the minimization of spectral leakage becomes the minimization of $\hat{\mathbf{d}}^\dagger \mathbf{F}^T \mathbf{Q} \mathbf{F}\hat{\mathbf{d}}$. As the product matrix $\mathbf{F}^T \mathbf{Q} \mathbf{F}$ is positive semi definite, the objective function $\hat{\mathbf{d}}^\dagger \mathbf{F}^T \mathbf{Q} \mathbf{F}\hat{\mathbf{d}}$ can be minimized by choosing $\hat{\mathbf{d}}$ to be the eigen vector corresponding to the smallest eigen value of

$\mathbf{F}^T \mathbf{Q} \mathbf{F}$. As the matrix $\mathbf{F}^T \mathbf{Q} \mathbf{F}$ is real, the optimal window also has real coefficients. Notice that the resulting window is different from the solution obtained in [16]. In [16], the window is derived subject to the constraint that the window is the inverse of a raised cosine function.

Symmetry of the Window: The solution of the optimal window \mathbf{d} obtained can be shown to be symmetric under a very mild assumption. To see that, let the smallest eigen value of $\mathbf{F}^T \mathbf{Q} \mathbf{F}$ be λ and the associated eigen vector be \mathbf{v} , i.e.,

$$\mathbf{F}^T \mathbf{Q} \mathbf{F} \mathbf{v} = \lambda \mathbf{v}. \quad (18)$$

We assume the multiplicity of λ is one and $\lambda \neq 0$. Let \mathbf{J} denote the $N \times N$ reversal matrix. For example, the 3 by 3 reversal matrix is given by

$$\mathbf{J} = \begin{pmatrix} 0 & 0 & 1 \\ 0 & 1 & 0 \\ 1 & 0 & 0 \end{pmatrix}.$$

We observe that \mathbf{Q} has the property that $\mathbf{Q} = \mathbf{J} \mathbf{Q} \mathbf{J}$. In addition, by direct multiplication, we can verify that

$$\mathbf{J} \mathbf{F} \mathbf{F}^T \mathbf{J} = \mathbf{F} \mathbf{F}^T.$$

By multiplying the both sides of (18) by \mathbf{F} , we obtain

$$\mathbf{F} \mathbf{F}^T \mathbf{Q} (\mathbf{F} \mathbf{v}) = \lambda (\mathbf{F} \mathbf{v}). \quad (19)$$

This means that $\mathbf{F} \mathbf{v}$ is the eigen vector of $\mathbf{F} \mathbf{F}^T \mathbf{Q}$ associated with λ . Multiplying (19) by \mathbf{J} and using $\mathbf{Q} = \mathbf{J} \mathbf{Q} \mathbf{J}$, we can obtain $(\mathbf{J} \mathbf{F} \mathbf{F}^T \mathbf{J}) \mathbf{Q} \mathbf{J} \mathbf{F} \mathbf{v} = \lambda \mathbf{J} \mathbf{F} \mathbf{v}$. If we use the property $\mathbf{J} \mathbf{F} \mathbf{F}^T \mathbf{J} = \mathbf{F} \mathbf{F}^T$, then we arrive at the following equation:

$$\mathbf{F} \mathbf{F}^T \mathbf{Q} (\mathbf{J} \mathbf{F} \mathbf{v}) = \lambda (\mathbf{J} \mathbf{F} \mathbf{v}).$$

This means that $\mathbf{J} \mathbf{F} \mathbf{v}$ is also an eigen vector of $\mathbf{F} \mathbf{F}^T \mathbf{Q}$ associated with λ . Because the multiplicity of the eigen value λ is one and the energy of $\mathbf{F} \mathbf{v}$ is the same as that of $\mathbf{J} \mathbf{F} \mathbf{v}$, we observe that $\mathbf{F} \mathbf{v}$ and $\mathbf{J} \mathbf{F} \mathbf{v}$ are related by $\mathbf{F} \mathbf{v} = \pm \mathbf{J} \mathbf{F} \mathbf{v}$. Notice that $\mathbf{J} (\mathbf{F} \mathbf{v})$ is the flipped version of the window $\mathbf{F} \mathbf{v}$, i.e., $[\mathbf{J} (\mathbf{F} \mathbf{v})]_i = [\mathbf{F} \mathbf{v}]_{N-1-i}$ for $i = 0, 1, \dots, N-1$. The relation $\mathbf{F} \mathbf{v} = \pm \mathbf{J} \mathbf{F} \mathbf{v}$ implies that $\mathbf{F} \mathbf{v}$ is symmetric or antisymmetric. Note that the antisymmetric property leads to a zero at $\omega = 0$ [17]. As our desired window is a lowpass filter, we can conclude that the window is symmetric. Therefore, in this case, the window has both cyclic-prefixed property and symmetry property. Combining these two properties, we can further deduce that the first L coefficients of the window satisfy $d_i = d_{L-1-i}$ for $i = 0, 1, \dots, L-1$.

To incorporate SNR in the optimization, we can form the objective function

$$\phi = c \hat{\mathbf{d}}^T \mathbf{F}^T \mathbf{Q} \mathbf{F} \hat{\mathbf{d}} + (1-c) \sum_{k=0}^{M-1} \frac{1}{|d_k|^2} \quad (20)$$

where $0 \leq c \leq 1$. In this case, the objective function is no longer in quadratic form. Nonlinear optimization packages can be used to design the window, e.g., [19]. The parameter c gives a tradeoff between spectral leakage and SNR.

Example 1—Windowed DFT-Based Transceiver With Cyclic Prefix: The block size $M = 512$, and prefix length $L = 32$. We form the positive semi definite matrix $\mathbf{F}^T \mathbf{Q} \mathbf{F}$ and compute

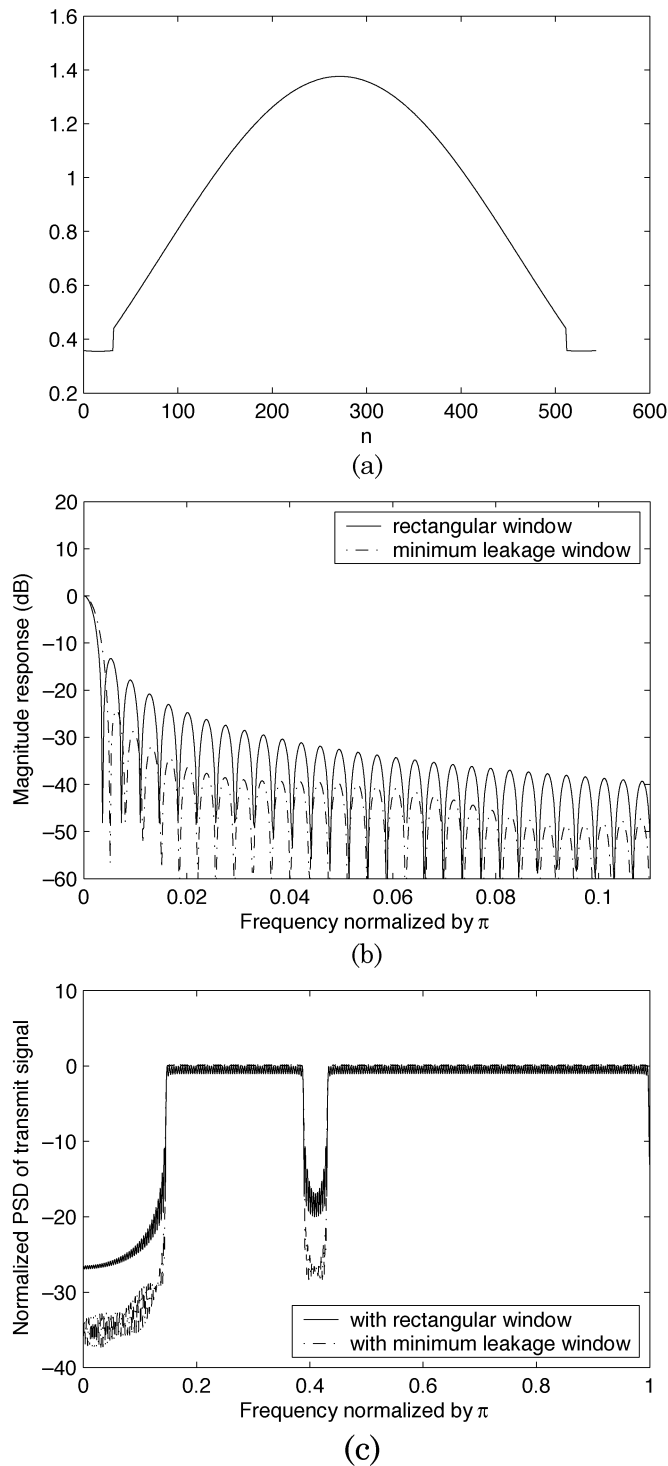


Fig. 5. Example 1. Windows for cyclic-prefixed transceivers. (a) Time-domain plot of the window with minimum spectral leakage. (b) Magnitude response of the window in (a). (c) Power spectral density of the transmit signal.

the eigen vector corresponding to the smallest eigen value to obtain $\hat{\mathbf{d}}$. The resulting window \mathbf{d} is as shown in Fig. 5(a). The magnitude response of $D(e^{j\omega})$ is shown in Fig. 5(b). Fig. 5(c) shows the spectrum of the transmitter output using the window in Fig. 5(a). The subcarriers used are 38 to 99 and 111 to 255, as in [16]. The subcarriers with indices smaller than 38 are reserved for voice band and upstream transmission, and those with indices between 99 and 111 are for egress control. We see that

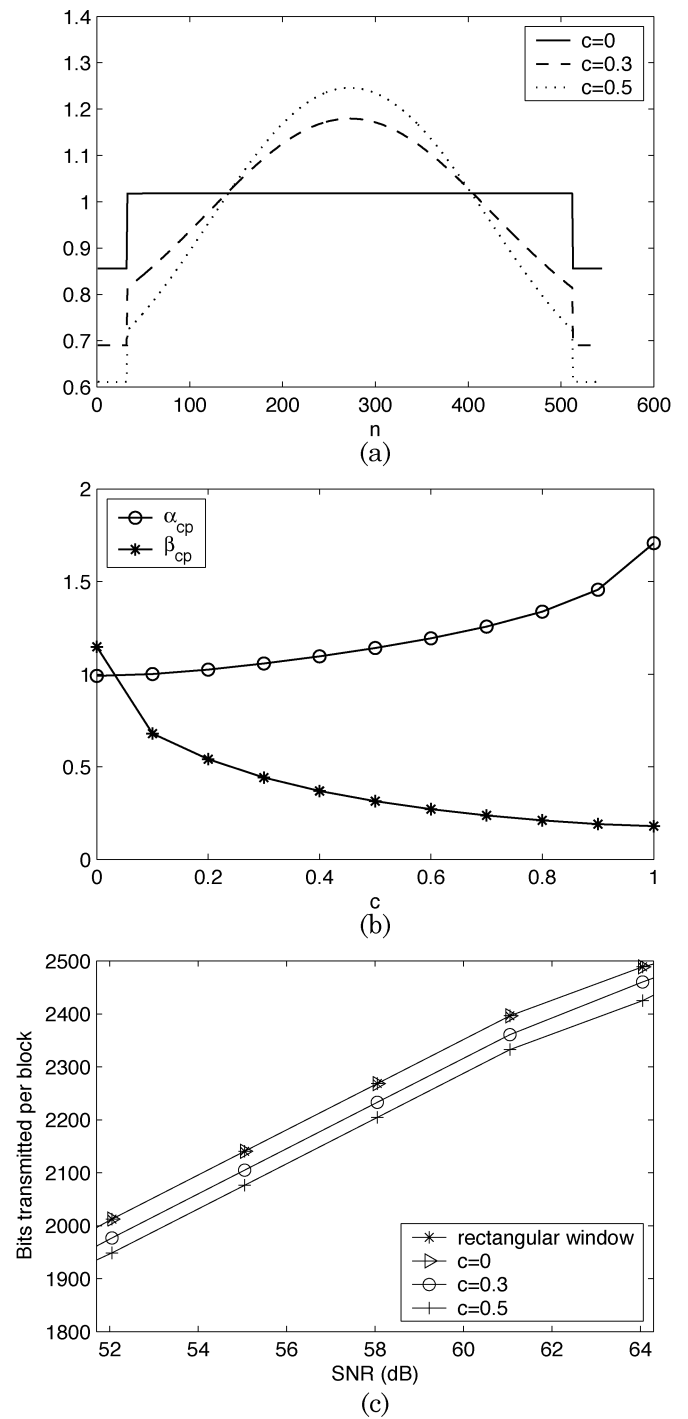


Fig. 6. Example 2. Joint optimization for cyclic-prefixed transceivers. (a) Windows obtained by joint optimization of spectral leakage and SNR. (b) Spectral leakage β_{cp} and SNR loss α_{cp} versus the trade-off factor c . (c) Performances of windowed transceivers.

the spectrum of the windowed output has a much smaller spectral leakage in unused bands.

Example 2—Joint Optimization, Cyclic Prefix Case: Using the nonlinear optimization package in [19], we optimize the window to minimize the objective function in (20) that incorporates both spectral leakage and SNR. The resulting windows \mathbf{d} for $c = 0, 0.3$, and 0.5 are as shown in Fig. 6(a). Fig. 6(b) shows α_{cp} and β_{cp} versus the trade-off factor c . For example, when $c = 0.3$, spectral leakage β_{cp} is 0.4, and α_{cp} is 1.1 (0.41 dB).

Different values of c give us a different tradeoff between spectral leakage and SNR. As c increases, we get a smaller spectral leakage β_{cp} at the price of a larger SNR loss. Observe that when $c = 0$, the objective function becomes SNR loss only. The resulting window has SNR loss $\alpha_{cp} = 0.99$: slightly less than 1.

Fig. 6(c) shows the transmission rate when the symbol error rate is fixed at 10^{-4} . The input s_k are QAM modulation symbols, and subchannel SNRs are used to determine bit allocation. We have used the same set of subcarriers in Fig. 5(c). The windows are designed using $c = 0, 0.3$, and 0.5 . The channel used in the simulation is Loop 6, which is a typical channel in carrier serving area [2], and the channel noise is AWGN. Fig. 6(c) shows the number of bits transmitted per block. For example, when SNR = 58 dB, 2233 bits, and 2204 bits per block are transmitted, respectively, for $c = 0.3$ and $c = 0.5$. Compared with 2268 bits per block for the rectangular window, the rate losses are only around 1.6% and 2.8%, respectively. For $c = 0$, the result is virtually the same as that of the rectangular window.

B. Windows for Zero-Padded Systems

For the zero-padded system, Lemma 2 shows that the postprocessing matrix is channel independent for any choice of window $\mathbf{d} = (d_0 d_1 \cdots d_{M-1})^T$. Similar to the cyclic-prefixed case, the Fourier transform of the window function can be expressed as

$$D(e^{j\omega}) = \mathbf{e}(e^{j\omega})\mathbf{K}\mathbf{d}, \quad \text{where } \mathbf{K} = \begin{pmatrix} \mathbf{I}_M \\ \mathbf{0} \end{pmatrix}$$

and the vector $\mathbf{e}(e^{j\omega})$ is as in (16).

Using derivations similar to those for the cyclic-prefixed case, the stopband energy of the window can be written as

$$\mathcal{S} = \mathbf{d}^\dagger \mathbf{K}^T \mathbf{Q} \mathbf{K} \mathbf{d}$$

where \mathbf{Q} is as given in (17). As the matrix $\mathbf{K}^T \mathbf{Q} \mathbf{K}$ is real, symmetric, and positive semi definite, we can find the optimal window by computing the eigen vector corresponding to the smallest eigen value. One can show that the optimal window is real and symmetric by following a procedure similar to the cyclic prefix case. We can also use the objective function

$$\phi = \mathbf{c} \mathbf{d}^T \mathbf{K}^T \mathbf{Q} \mathbf{K} \mathbf{d} + (1 - c) \sum_{k=0}^{M-1} \frac{1}{|d_k|^2} \quad (21)$$

to incorporate SNR in the design. When $c = 0$, the window is optimized to minimize the SNR loss $\sum_{k=0}^{M-1} (1/|d_k|^2)$. Notice that the function $1/x$ is convex, which implies

$$\frac{1}{M} \sum_{k=0}^{M-1} \frac{1}{|d_k|^2} \geq \frac{1}{\frac{1}{M} \sum_{k=0}^{M-1} |d_k|^2} = 1. \quad (22)$$

Using the above inequality, we see that the optimal solution when $c = 0$ becomes the rectangular window.

Example 3—Windowed DFT-based Transceiver With Zero Padding: As in earlier examples, we choose $M = 512$ and $L = 32$. Like the cyclic-prefixed case, we use the nonlinear optimization package in [19] to optimize the window so that the objective function given in (21) is minimized. The resulting windows for $c = 0, 0.2$ and 0.5 are as shown in Fig. 7(a). Notice that the window corresponding to $c = 0$ is the rectangular window, as we have expected. The magnitude responses of the windows in Fig. 7(a) are shown in Fig. 7(b). The windows

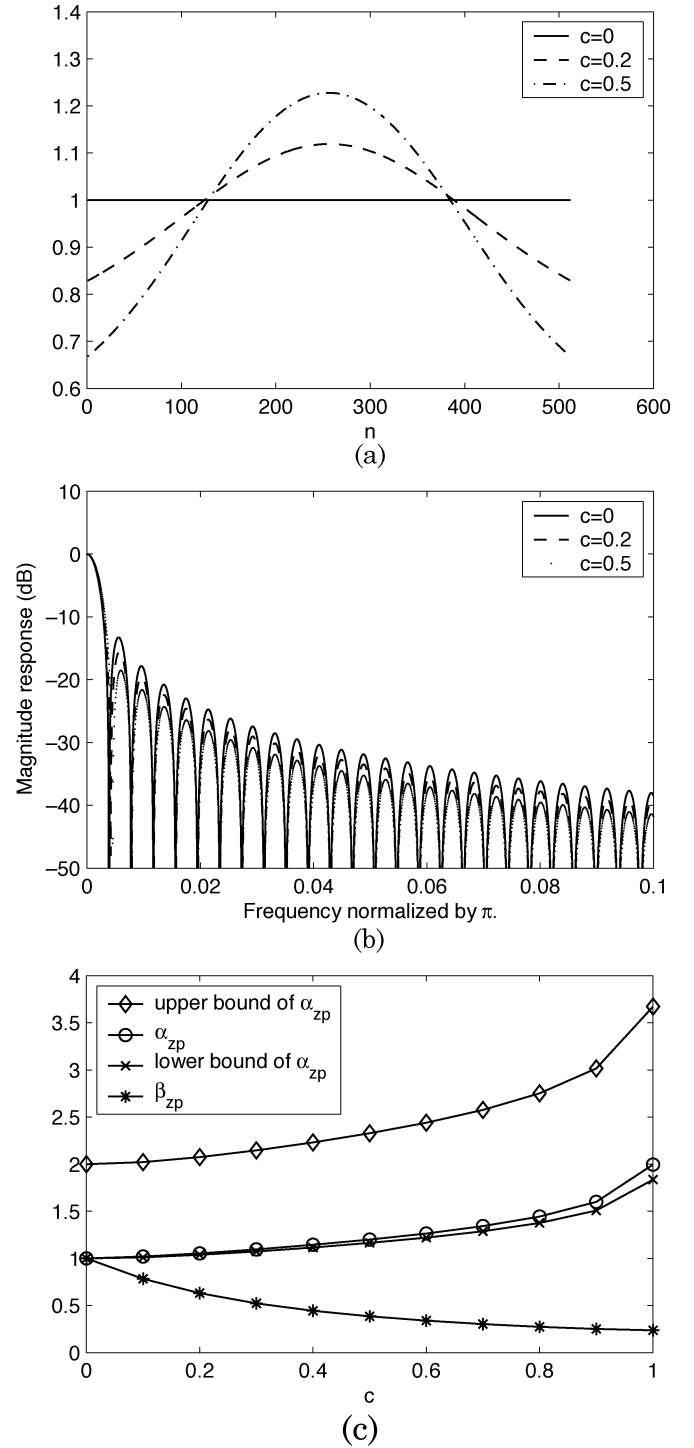


Fig. 7. Example 3. Windows for zero-padded transceivers. (a) Windows obtained by joint optimization of spectral leakage and SNR. (b) Magnitude response of the window in (a). (c) Spectral leakage β_{zp} , α_{zp} , lower bound and upper bound of α_{zp} versus the tradeoff factor c .

correspond to larger c have better stopband attenuation and hence smaller spectral leakage.

Fig. 7(c) shows β_{zp} for different trade-off factor c . For the zero-padded transceiver, α_{zp} is channel dependent. To plot α_{zp} , we use a random channel of 32 taps, where each tap is an independent Gaussian random variable with unit variance, and a total of 10 000 channel realizations are used. The channel noise is AWGN. The average α_{zp} from all the channel realizations is

as given in Fig. 7(c). The upper bound and lower bound of α_{zp} in (15) are also given in the same plot for comparison. The gap between α_{zp} and the lower bound is very small. Similar to the cyclic-prefixed case, we can obtain a tradeoff between SNR and spectral leakage for different c .

V. CONCLUSIONS

In this paper, we considered windowed DFT-based multicarrier systems with cyclic prefix and with zero padding. The spectral leakage of the transmit signal can be reduced significantly by using windows. Like earlier works of windowed transceivers, the use of windows at the transmitter side requires postprocessing at the receiver side, which is usually channel dependent. We show that for the cyclic-prefixed system with a zero-forcing receiver, postprocessing is channel independent if the window itself has cyclic-prefixed property. For both cyclic-prefixed and zero-padded systems, the optimal window that minimizes spectral leakage of the transmit signal can be given in closed forms. We also show that postprocessing affects the output SNR. The output SNR can be given in terms of the window and the channel. Furthermore, for both cyclic-prefixed and zero-padded systems with windowing, we can jointly optimize spectral leakage and SNR. The results show that these window designs provide a good tradeoff between SNR and spectral leakage.

APPENDIX PROOF OF LEMMA 1

As there is no interblock interference, we only need to consider intrablock interference, and the transfer function of the system from the transmitter input to the receiver output is a constant matrix \mathbf{T} . Using \mathbf{G}_{cp} and \mathbf{S}_{cp} given in (3), the overall transfer matrix \mathbf{T} is

$$\mathbf{T} = \mathbf{P}_{cp} \mathbf{A} \mathbf{W} \mathbf{H} \mathbf{D}_{cp} \begin{pmatrix} \mathbf{0} & \mathbf{I}_L \\ \mathbf{I}_M & \mathbf{0} \end{pmatrix} \mathbf{W}^\dagger$$

where the matrix \mathbf{H} is of dimensions $M \times N$. It is Toeplitz with the first row given by $(c_L c_{L-1} \cdots c_0 0 \cdots 0)$. With the partition of \mathbf{D}_{cp} in (4), we have

$$\mathbf{T} = \mathbf{P}_{cp} \mathbf{A} \mathbf{W} \mathbf{H} \begin{pmatrix} \mathbf{0} & \mathbf{D}_0 \\ \mathbf{D}_1 & \mathbf{0} \\ \mathbf{0} & \mathbf{D}_2 \end{pmatrix} \mathbf{W}^\dagger.$$

Let us partition \mathbf{H} as

$$\mathbf{H} = \begin{pmatrix} \mathbf{C}_0 & \mathbf{C}_1 & \mathbf{0} \\ \mathbf{0} & \mathbf{C}_1 & \mathbf{C}_2 \end{pmatrix}$$

where \mathbf{C}_0 and \mathbf{C}_2 are of dimensions $L \times L$, and \mathbf{C}_1 is $M \times (M - L)$. The matrix \mathbf{T} can be written as

$$\mathbf{T} = \mathbf{P}_{cp} \mathbf{A} \mathbf{W} \begin{pmatrix} \mathbf{C}_1 \mathbf{D}_1 & \mathbf{C}_0 \mathbf{D}_0 \\ \mathbf{C}_2 \mathbf{D}_2 & \mathbf{0} \end{pmatrix} \mathbf{W}^\dagger \quad (23)$$

$$= \mathbf{P}_{cp} \mathbf{A} \mathbf{W} \left[\begin{pmatrix} \mathbf{C}_1 \mathbf{D}_1 & \mathbf{C}_0 \mathbf{D}_2 \\ \mathbf{C}_2 \mathbf{D}_2 & \mathbf{0} \end{pmatrix} + \begin{pmatrix} \mathbf{0} & \mathbf{C}_0 (\mathbf{D}_0 - \mathbf{D}_2) \\ \mathbf{0} & \mathbf{0} \end{pmatrix} \right] \mathbf{W}^\dagger \quad (24)$$

$$= \mathbf{P}_{cp} \mathbf{A} \mathbf{W} \left[\underbrace{\begin{pmatrix} \mathbf{C}_1 & \mathbf{C}_0 \\ \mathbf{C}_2 & \mathbf{0} \end{pmatrix}}_{\mathbf{C}} \begin{pmatrix} \mathbf{D}_1 & \mathbf{0} \\ \mathbf{0} & \mathbf{D}_2 \end{pmatrix} + \begin{pmatrix} \mathbf{0} & \mathbf{C}_0 (\mathbf{D}_0 - \mathbf{D}_2) \\ \mathbf{0} & \mathbf{0} \end{pmatrix} \right] \mathbf{W}^\dagger. \quad (25)$$

The matrix \mathbf{C} is an $M \times M$ circulant matrix, and by (2), it can be factorized as $\mathbf{W}^\dagger \mathbf{\Gamma} \mathbf{W}$, where $\mathbf{\Gamma} = \mathbf{\Lambda}^{-1}$. We arrive at the following expression for \mathbf{T} :

$$\mathbf{T} = \mathbf{P}_{cp} \left[\mathbf{W} \begin{pmatrix} \mathbf{D}_1 & \mathbf{0} \\ \mathbf{0} & \mathbf{D}_2 \end{pmatrix} \mathbf{W}^\dagger + \mathbf{A} \mathbf{W} \begin{pmatrix} \mathbf{0} & \mathbf{C}_0 (\mathbf{D}_0 - \mathbf{D}_2) \\ \mathbf{0} & \mathbf{0} \end{pmatrix} \mathbf{W}^\dagger \right].$$

For a zero-forcing solution, \mathbf{P}_{cp} is the inverse of the matrix in the bracket. △△△

ACKNOWLEDGMENT

The authors would like to thank Y.-Y. Jian, C.-C. Su, and P.-J. Chung for performing the simulations.

REFERENCES

- [1] L. J. Cimini, "Analysis and simulation of a digital mobile channel using orthogonal frequency division multiplexing," *IEEE Trans. Commun.*, vol. COM-33, pp. 665–675, Jul. 1985.
- [2] *Asymmetric Digital Subscriber Lines (ADSL)-Metallic Interface*, ANSI T1.413, 1998.
- [3] *Very-High Speed Digital Subscriber Lines (VDSL)-Metallic Interface*, ANSI T1.424, 2002.
- [4] *ISO/IEC*, IEEE Std. 802.11a, 1999.
- [5] *ETSI Digital Video Broadcasting; Framing, Structure, Channel Coding and Modulation for Digital Terrestrial Television (DVB-T)*, ETS 300 744, 1997.
- [6] A. Vahlin and N. Holte, "Optimal finite duration pulses for OFDM," *IEEE Trans. Commun.*, vol. 44, no. 1, pp. 10–14, Jan. 1996.
- [7] H. Nikookar and R. Prasad, "Optimal waveform design for multicarrier transmission through a multipath channel," in *Proc. IEEE Vehicular Tech. Conf.*, vol. 3, May 1997, pp. 1812–1816.
- [8] K. Matheus and K.-D. Kammeyer, "Optimal design of a multicarrier systems with soft impulse shaping including equalization in time or frequency direction," in *Proc. IEEE Global Telecommun. Conf.*, vol. 1, Nov. 1997, pp. 310–314.
- [9] N. Laurenti and L. Vangelista, "Filter design for the conjugate OFDM-OQAM system," in *Proc. First Int. Workshop Image Signal Processing Analysis*, Jun. 2000.
- [10] S. B. Slimane, "Performance of OFDM systems with time-limited waveforms over multipath radio channels," in *Proc. Global Telecommun. Conf.*, 1998.
- [11] Y.-P. Lin and S.-M. Phoong, "OFDM transmitters: analog representation and DFT-based implementation," *IEEE Trans. Signal Process.*, vol. 51, no. 9, pp. 2450–2453, Sep. 2003.
- [12] R. W. Lowdermilk, "Design and performance of fading insensitive orthogonal frequency division multiplexing (OFDM) using polyphase filtering techniques," in *Conf. Rec. Thirtieth Asilomar Conf. Signals, Syst. Comput.*, Nov. 1996.
- [13] H. Boelcskei, P. Duhamel, and R. Hleiss, "Design of pulse shaping OFDM/OQAM systems for high data-rate transmission over wireless channels," in *Proc. IEEE Int. Conf. Commun.*, 1999.
- [14] P. Siohan, C. Siclet, and N. Lacaille, "Analysis and design of OFDM/OQAM systems based on filterbank theory," *IEEE Trans. Signal Processing*, vol. 50, no. 5, pp. 1170–1183, May 2002.
- [15] M. Pauli and P. Kuchenbecker, "On the reduction of the out-of-band radiation of OFDM-signals," in *Proc. IEEE Int. Conf. Commun.*, vol. 3, Jun. 1998, pp. 1304–1308.
- [16] G. Cuypers, K. Vanbleu, G. Ysebaert, M. Moonen, and P. Vandaele, "Combining raised cosine windowing and per tone equalization for RFI mitigation in DMT receivers," in *Proc. IEEE Int. Conf. Commun.*, 2003.

- [17] A. V. Oppenheim and R. W. Schaffer, *Discrete-Time Signal Processing*, Second ed. Englewood Cliffs, NJ: Prentice-Hall, 1999.
- [18] J. G. Proakis, *Digital Communications*. New York: McGraw-Hill, 1995.
- [19] W. H. Press, B. P. Flannery, S. A. Teukolsky, and W. T. Vetterling, *Numerical Recipes*. Cambridge, U.K.: Cambridge Univ. Press, 1989.



Yuan-Pei Lin (S'93–M'97–SM'03) was born in Taipei, Taiwan, R.O.C., in 1970. She received the B.S. degree in control engineering from the National Chiao-Tung University, Hsinchu, Taiwan, in 1992, and the M.S. and Ph.D. degrees, both in electrical engineering, from the California Institute of Technology, Pasadena, in 1993 and 1997, respectively.

She joined the Department of Electrical and Control Engineering, National Chiao-Tung University, in 1997. Her research interests include digital signal processing, multirate filterbanks, and digital

communication systems with emphasis on multicarrier transmission.

Dr. Lin is currently an associate editor for IEEE TRANSACTIONS ON SIGNAL PROCESSING and an associate editor for the Academic Press journal *Multidimensional Systems and Signal Processing*.



See-May Phoong (M'96–SM'03) was born in Johor, Malaysia, in 1968. He received the B.S. degree in electrical engineering from the National Taiwan University (NTU), Taipei, Taiwan, R.O.C., in 1991 and the M.S. and Ph.D. degrees in electrical engineering from the California Institute of Technology (Caltech), Pasadena, in 1992 and 1996, respectively.

He was with the Faculty of the Department of Electronic and Electrical Engineering, Nanyang Technological University, Singapore, from September 1996 to September 1997. In September 1997, he joined the

Graduate Institute of Communication Engineering and the Department of Electrical Engineering, NTU, as an Assistant Professor, and since August 2001, he has been an Associate Professor. His interests include multirate signal processing and filterbanks and their application to communications.

Dr. Phoong is currently an Associate Editor for the IEEE SIGNAL PROCESSING LETTERS. He served as an Associate Editor for the IEEE TRANSACTIONS ON CIRCUITS AND SYSTEMS II from January 2002 to December 2003. He received the Charles H. Wilts Prize in 1997 for outstanding independent research in electrical engineering at Caltech.